



Semiconductor superlattices with periodic disorder

H. X. Jiang and J. Y. Lin

Citation: *Journal of Applied Physics* **63**, 1984 (1988); doi: 10.1063/1.341098

View online: <http://dx.doi.org/10.1063/1.341098>

View Table of Contents: <http://scitation.aip.org/content/aip/journal/jap/63/6?ver=pdfcov>

Published by the [AIP Publishing](#)



Re-register for Table of Content Alerts

Create a profile.



Sign up today!



Semiconductor superlattices with periodic disorder

H. X. Jiang

Center for Fundamental Materials Research and Department of Physics and Astronomy,
Michigan State University, East Lansing, Michigan 48824-1116

J. Y. Lin

Department of Physics, Syracuse University, Syracuse, New York 13244-1130

(Received 30 September 1987; accepted for publication 23 November 1987)

For a real superlattice, fluctuations are always presented in the period lengths. The band structure of semiconductor superlattices under the effect of this periodic disorder has been investigated in this paper. The zone center and zone edge of the first subband of electrons and holes and the effective energy gap as functions of this fluctuation have been calculated. We discuss the dependence of the band offset on this fluctuation. Our calculated results can be used to explain some of the experimental observations.

I. INTRODUCTION

Advances in epitaxial crystal growth techniques such as molecular-beam epitaxy (MBE) and metalorganic chemical vapor deposition (MOCVD) enabled the fabrication of new metastable structures with controlled thicknesses and sharp interfaces.^{1,2} Superlattices are a special class of these novel structures which are finding increasing applications, not only in applied areas such as lasers, but also in basic research areas such as the study of electrons and holes in quasi-two-dimensional systems. Another interesting property of the superlattice is the formation of minibands. There are numerous published articles in this field.³⁻⁵ The most extensively studied superlattice is the one consisting of alternate layers of GaAs and Ga_{1-x}Al_xAs.

Although it is commonly accepted that MBE is capable of fabricating interfaces between two semiconductors to grow quantum wells (QWs) and superlattices with very high quality, one can never grow superlattices with the ideal structure. Here, an ideal superlattice means an array of two (or more) alternating layers of materials with a single period, fixed well (barrier) width and barrier height, no roughness on the interfaces, and infinitely abrupt interfaces. A real superlattice differs from an ideal one in many aspects. They include: (a) unsharp interfaces, or band bending in the depletion regions; (b) interface disorder or roughness, or thickness fluctuations within a quantum well (barrier); (c) fluctuations in the average thickness of the well (barrier) width from layer to layer; and (d) fluctuations in the potential barrier height. The band structure of realistic superlattices have been investigated briefly in a previous paper.⁶

The effect of layer thickness fluctuations to the superlattice diffraction pattern has been recently investigated by Clemens and Gay.⁷ Two types of fluctuation distributions were considered: continuous random fluctuations which result from disorder or amorphous interfaces and discrete fluctuations resulting from coherent interfaces. They presented numerical simulations of diffraction from multilayers constructed by either type of fluctuation.

In general, all the results for the miniband structures of superlattices were obtained under the assumption that superlattices are the perfect periodic structures (no fluctuations in the period lengths). For a real superlattice, since

the open/close timing of shutter for deposition is controlled only by a clock, there are always fluctuations in the widths of quantum wells and barriers, and consequently in the superlattice period lengths, and we shall name this the periodic disorder. These fluctuations depend on the growth conditions and are different from sample to sample. The periodic disorder has been mentioned previously by a few other groups who claimed that it is one of the reasons for the linewidth broadening in the optical experiments. Although the reason for the linewidth broadening is believed mainly due to interface disorder, or fluctuation within a quantum well or barrier.⁸⁻¹⁰ The band structure of a superlattice under the effect of this type of disorder has never been studied in detail before. In this paper, we calculated dependencies of the band structures and the effective energy gap of Ga_{1-x}Al_xAs-GaAs superlattice on the fluctuation. The results obtained are useful in device applications and in basic research.

II. CALCULATIONS

Figure 1 is the configuration (top) and the band profile (bottom) of the superlattice with periodic disorder. In Fig. 1, $a_i = a_0 + \delta_i^a$ and $b_i = b_0 + \delta_i^b$ are the widths of the quantum barrier and well, respectively, in the i th "period." a_0 (b_0) is the average width of the quantum barrier (well)

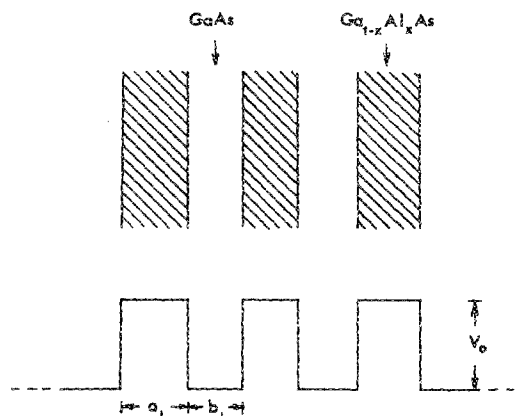


FIG. 1. The configuration (top) and the band profile (bottom) of the Ga_{1-x}Al_xAs-GaAs superlattice with periodic disorder.

$\delta_i^a(\delta_i^b)$ is the small fluctuation in the barrier (well) width in the i th period.

$$L_i = L_o + \delta_i^+ (\delta_i^+ = \delta_i^a + \delta_i^b),$$

is the i th "effective period length" and $L_o = a_o + b_o$ is the overall average "period length." Because the fluctuations are random, when n is large, we should have

$$\sum_{i=1}^n L_i = nL_o,$$

where n is the total number of periods. We assume that the fluctuations in the quantum well (barrier) widths δ_i (δ_i^a and δ_i^b) have the Gaussian distribution

$$P(\delta_i) = N \exp(-\delta_i^2/2\sigma^2), \quad (1)$$

where N is the normalization constant. σ is the fluctuation parameter which depends on the growth conditions and varies from sample to sample. Therefore, we have

$$\sum_{i=1}^n \delta_i^a = \sum_{i=1}^n \delta_i^b = 0.$$

For a real superlattice, there is only a finite number of layers. We assume that the wave functions of electrons and holes have the cyclic boundary condition at the two boundaries

$$\psi(x=0) = \psi\left(x = \sum_{i=1}^n L_i\right). \quad (2)$$

In the calculation, instead of δ_i varying continuously, we consider discrete fluctuations. δ_i has been taken from 0 to $\pm 3 \text{ \AA}$ with step 0.5 \AA and following the distribution of Eq. (1). Thus, we have

$$N = \left[1 + 2 \sum_{m=1}^3 \exp\left(\frac{-d^2 m^2}{2\sigma^2}\right)\right]^{-1}, \quad (3)$$

where d is some plane spacing of the layer and has been taken as 0.5 \AA in this paper. For simplicity, δ_i has been limited within 3 \AA . In the real case, it should change for different samples. However, the results obtained here can represent the cases of the real superlattice systems.

The potential form for the electrons and holes can be written as

$$V(x) = \begin{cases} 0, & 0 < x - x_n < a_{n+1}, \\ V, & a_{n+1} < x - x_n < L_{n+1}, \end{cases} \quad (4)$$

$n = 0, 1, 2, \dots$, where $x_n = \sum_{i=1}^n L_i$. From the Schrödinger equation

$$\left(\frac{-\hbar^2}{2m}\right) \frac{d^2\psi}{dx^2} + V\psi = E\psi, \quad (5)$$

we can immediately get the wave function in the n th period as

$$\psi(x) = \begin{cases} A_n \exp(ikx) + B_n \exp(-ikx) & \text{(in the well of } n\text{th period),} \\ C_n \exp(Kx) + D_n \exp(-Kx) & \text{(in the barrier of } n\text{th period),} \end{cases} \quad (6)$$

where A_n, B_n, C_n , and D_n are the constant coefficients of the wave function in the n th period.

Using the transfer-matrix method,^{11,12} and the continuity conditions of $\psi(x)$ and $(1/m)(d\psi/dx)$ across the in-

terfaces, we get the following expression:

$$\begin{pmatrix} A_n \\ B_n \end{pmatrix} = M_n \begin{pmatrix} A_{n-1} \\ B_{n-1} \end{pmatrix} = \prod_{i=1}^n M_i \begin{pmatrix} A_o \\ B_o \end{pmatrix}, \quad (7)$$

where $M_i = P_i Q_i$ and

$$P_i = \begin{pmatrix} \alpha_i - i\beta_i & -i\gamma_i \\ i\gamma_i & \alpha_i + i\beta_i \end{pmatrix}, \quad (8)$$

$$Q_i = \begin{pmatrix} \exp(ikL_i) & \\ & \exp(-ikL_i) \end{pmatrix}; \quad (9)$$

$$\begin{aligned} K\alpha_i &= \cosh(Ka_i)\cos(ka_i) - (\epsilon/2)\sinh(Ka_i)\sin(ka_i), \\ \beta_i &= \cosh(Ka_i)\sin(ka_i) + (\epsilon/2)\sinh(Ka_i)\cos(ka_i), \\ \gamma_i &= (\eta/2)\sinh(Ka_i), \end{aligned} \quad (10)$$

and

$$\begin{aligned} \epsilon &= (m_1 K / m_2 k) - (m_2 k / m_1 K), \\ \eta &= (m_1 K / m_2 k) + (m_2 k / m_1 K), \\ k &= \sqrt{2m_1 E} / \hbar \text{ and } K = \sqrt{2m_2(V - E)} / \hbar. \end{aligned} \quad (11)$$

E is the energy of the electron (hole); m_1 and m_2 are, respectively, the effective masses in the well and barrier materials, and $V = V_e$ or (V_h) is the the height of the potential barrier for electrons (or holes).

From Eqs. (2) and (7), we can get the dispersion relations as the following:

$$\cos(qL) = \frac{1}{2} \text{Tr}(M), \quad (12)$$

where $M = \prod_{i=1}^n M_i$ and L is the overall length of the super-

lattice $L = \sum_{i=1}^n L_i$. In the case of real superlattices, only a finite number of layers are involved. In this paper, we will let n , the total number of periods equal to 100 (except for Fig. 2).

III. RESULTS AND DISCUSSIONS

In our calculations, we have used $m_1 = 0.067 m_o$ for the electron effective mass for GaAs, $m_2 = (0.067 + 0.083x)m_o$

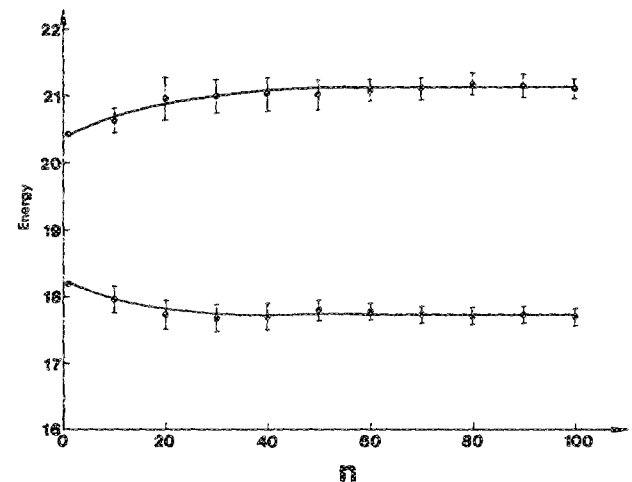


FIG. 2. Energy of the zone center (lower) and zone edge (upper) of the first conduction subband as functions of n , the total number of periods, with $\sigma = 1 \text{ \AA}$, $a_o = b_o = 50 \text{ \AA}$, and $x = 0.3$. In all figures, the energy of electrons is measured from the bottom of the quantum wells. The unit of the energy is $\hbar^2\pi^2/2m_oL^2 = 3.76 \text{ meV}$ with $L = 100 \text{ \AA}$.

for the electron mass in $\text{Ga}_{1-x}\text{Al}_x\text{As}$, and the empirical expression $E_g = 1.155x + 0.37x^2$ (eV) for the direct band-gap difference between GaAs and $\text{Ga}_{1-x}\text{Al}_x\text{As}$.¹³⁻¹⁵ The band gap of GaAs is 1.520 (eV).¹⁶ The conduction- and valence-band discontinuities at the interface have been suggested to be about 60% (Q_c) and 40% (Q_v), respectively, of the direct band-gap difference between the two semiconductor materials.^{17,18} Thus we have $V_c = Q_c E_g$ and $V_v = Q_v E_g$. The unit of energy in this paper is $\hbar^2 \pi^2 / 2m_0 L^2 = 3.76$ (meV) with $L = 100 \text{ \AA}$. The energy of electrons and holes is measured from the bottom of the quantum wells.

Figure 2 is the plot of energy of the zone center (lower) and zone edge (upper) of the first conduction subband as functions of n , the total number of periods, with $\sigma = 1 \text{ \AA}$, $a_o = b_o = 50 \text{ \AA}$, and $x = 0.3$. In obtaining Fig. 2, we have done the following: for each n , we generate ten independent groups of random a_i and b_i with δ_i^a and δ_i^b satisfying Eq. (1). From the results of these ten different groups, we get the average energy value and the standard deviation as shown in Fig. 2. All other results in this paper are obtained in the same way. The physical meaning for averaging of ten independent groups of a_i, b_i are twofold. First, because fluctuations are random, samples grown under the same conditions will still have different band structures. We can only get the average energy and the fluctuation about this average value. Second, a_i and b_i are the effective barrier and well widths in the i th period. Electrons and holes at different locations in the plane perpendicular to the growth direction, even in the same quantum well and barrier, see different a_i and b_i by means of the interface disorder.^{6,8,10}

Figure 2 shows the effects of the fluctuations on the first conduction subband of a superlattice for different values of n . Two interesting features are revealed by Fig. 2. First, the energy of the zone center (zone edge) of the first subband decreases (increases) as n increases from 1 to about $n = 50$. Then it remains as a constant as n increases to 100. Second, the standard deviations decrease as n increases ($n < 50$). As n goes from 50 to 100, standard deviations are almost the same. From Fig. 2, we can see that for $n = 100$, both the energy and the standard deviation approach constant values, so we may consider that a superlattice of $n = 100$ can represent the overall characteristics of a disordered superlattice with an arbitrary number of layers. Except for Fig. 2, all the results in this paper are obtained for $n = 100$.

The fluctuation in the well and barrier width can decrease (increase) the energy of zone center (zone edge) of the first conduction subband. The reason is that the energy of the center of band (edge of band) mostly depends on the thicker (narrower) wells. The fluctuation expands the well width in certain regions of $b_o(1 - \delta_{\max}^b) < b_i < b_o(1 + \delta_{\max}^b)$, where δ_{\max}^b is the maximum fluctuation in the well width. So the band width of the first conduction subband increases due to the existence of the fluctuation. Although in Fig. 2 we only show the conduction subband, the same behavior is expected for the heavy- and light-hole valence subbands. The zone center of the first conduction subband is the ground state of electrons, and is very important for the investigations of the electronic and optical properties. Because of the existence of the periodic disorder in real superlattice, the

energy gap (or energy of exciton lines) obtained from experiments is smaller than the calculated value which was obtained under the assumption of the perfect periodic structure.

To see how the periodic disorder affects the ground-state energy of electrons, Fig. 3 plots the distribution of electrons P as a function of the ground-state energy E for 500 randomly generated groups of a_i, b_i [δ_i^a and δ_i^b satisfy Eq. (1)] with $\sigma = 2 \text{ \AA}$, $a_o = b_o = 50 \text{ \AA}$, and $x = 0.3$. The average energy and the standard deviation is 17.22 ± 0.16 . Note that when $\sigma = 0$ (without the fluctuation), the ground-state energy is 18.22. The fluctuation decreases the ground-state energy by about one unit (3.76 meV). The interesting result is that the distribution of electrons is asymmetric about the peak position, so that the average energy is slightly less than the peak energy value. Measuring from the peak position, the tail in the high-energy side extends to about 0.3 units compared with the tail in the low-energy side, which extends to about 0.45 units. We assume $\{a_i^\pm, b_i^\pm\}$ is an arrangement of quantum wells and barriers, where $a_i^\pm = a_o \pm \delta_i^a$ and $b_i^\pm = b_o \pm \delta_i^b$. Because fluctuations are random, we have $P^+\{a_i^+, b_i^+\} = P^-\{a_i^-, b_i^-\}$. This means that if the probability of the arrangement $\{a_i^+, b_i^+\}$ is P^+ , then the probability of the arrangement, denoted by P^- , should be equal to P^+ . P^- is obtained by replacing a_i^+ and b_i^+ with a_i^- and b_i^- . However, the ground-state energy for these two configurations is different from Eq. (12) because of the noncommutativity of the matrix M_i ($M = \prod_{i=1}^n M_i$). The overall effect is that electrons favor the low-energy side, which implies that electrons favor the larger quantum wells.

Figure 4 is the plot of the ground-state energy of the electron as a function of the fluctuation parameter σ with $L_o = 100 \text{ \AA}$, $a_o = b_o = L_o/2$, and $x = 0.3$. We can see that the fluctuation causes a reduction in the ground-state energy of the electron. The shift of the ground-state energy increases as σ increases. The standard deviation of the ground-state

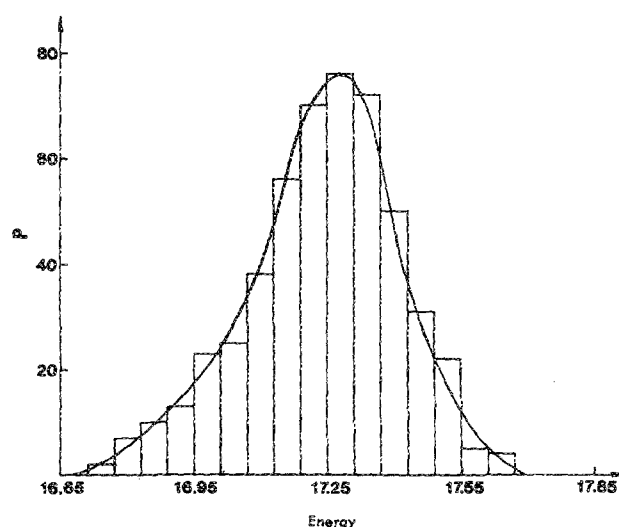


FIG. 3. The distribution of electrons P as a function of the ground-state energy E for 500 independent randomly generated groups of a_i, b_i with $\sigma = 2 \text{ \AA}$, $a_o = b_o = 50 \text{ \AA}$, and $x = 0.3$. The average energy value and the standard deviation in the ground state is 17.22 ± 0.16 .

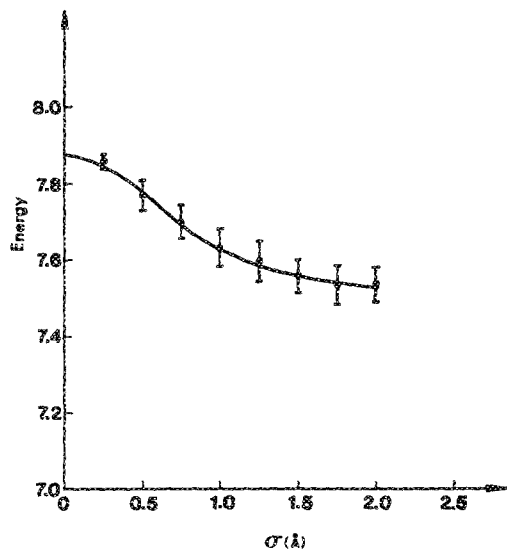


FIG. 4. Ground-state energy of electron as a function of fluctuation parameter σ with $L_0 = 200 \text{ \AA}$, $a_0 = b_0 = L_0/2$, and $x = 0.3$.

energy also increases as σ increases from 0 to 1 \AA . Then it remains constant as σ increases from 1 to 2 \AA . The ground-state energy decreases rapidly in the region of $\sigma = 0.5$ to 1.5 \AA . As σ increases from 0 to 2.0 \AA , the total reduction is about 0.35 unit (1.32 meV). This shift is related to the Mott's mobility edge.¹⁹ The importance of the result in Fig. 4 is that the ground-state energy can be varied from sample to sample even though the average well and barrier thicknesses remain constant.

Figure 5 is the plot of the ground-state energy of the electrons as a function of L_0 for three different fluctuation parameters $\sigma = 0, 1, \text{ and } 2 \text{ \AA}$ with $a_0 b_0 = L_0/2$ and $x = 0.3$. The inset shows the shift of the ground-state energy of the electrons, $E_{\sigma=0} - E_{\sigma=2}$ as a function of L_0 . As we can see from Fig. 5, the fluctuation decreases the ground-state energy of the electrons for all L_0 and the shift decreases as L_0 increases. For $L_0 = 40 \text{ \AA}$, the shifts between $E(\sigma = 2 \text{ \AA})$, $E(\sigma = 1 \text{ \AA})$, and $E(\sigma = 0)$ are 1.1 and 0.56 units, respectively. At $L_0 = 240 \text{ \AA}$, they are 0.29 and 0.21 units, respectively. A sharp decrease occurred at $L_0 = 120 \text{ \AA}$. Therefore, the same fluctuation has more effect at small L_0 . The standard deviation of energy decreases as L_0 increases as shown in the inset. The same behavior is expected for the heavy- and light-hole valence bands.

Figure 6 is the plot of the shift of the ground-state energy of electron $E_{\sigma=0} - E_{\sigma=1}$, and $E_{\sigma=0} - E_{\sigma=2}$, as functions of Al concentration x with $L_0 = 100 \text{ \AA}$ and $a_0 = b_0 = L_0/2$. In Fig. 6, we only present the average energy values from ten independent groups of a_i and b_i . The standard deviations are not indicated. The amount of the shift increases as x increases. This means that the fluctuation has more effect on the samples with higher Al concentrations. For small x ($x < 0.2$), the shift increases slowly for both $E_{\sigma=0} - E_{\sigma=2}$ and $E_{\sigma=0} - E_{\sigma=1}$. The sharp increases occur in the region of $0.2 \leq x \leq 0.6$ for both cases. The difference between $E_{\sigma=0} - E_{\sigma=1}$ and $E_{\sigma=0} - E_{\sigma=2}$ also increases as x increases.

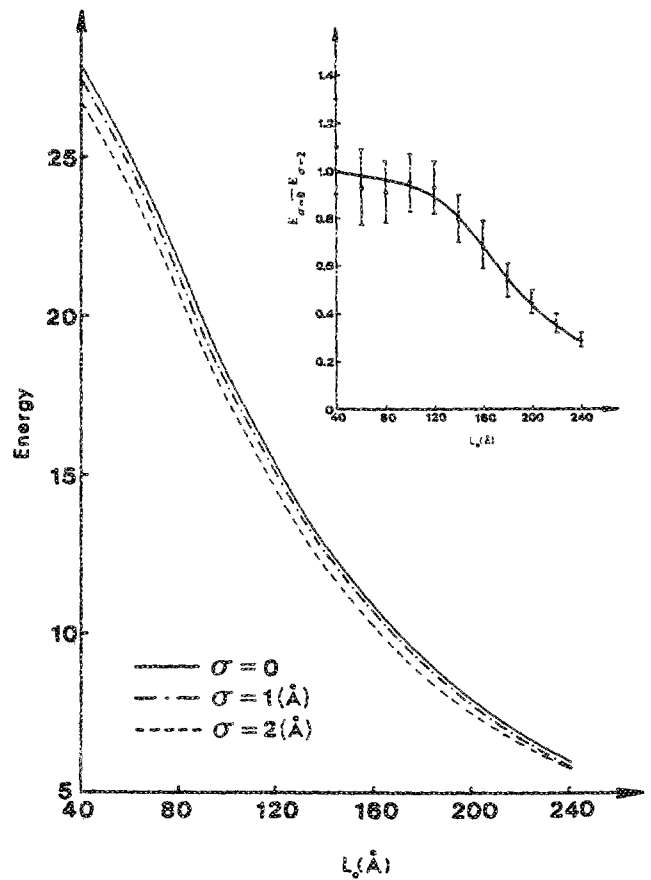


FIG. 5. Ground-state energy of electrons as a function of L_0 for three different values of fluctuation parameter σ with $a_0 = b_0 = L_0/2$, and $x = 0.3$. The inset is the shift of the ground-state energy of electrons $E_{\sigma=0} - E_{\sigma=2}$ as a function of L_0 .

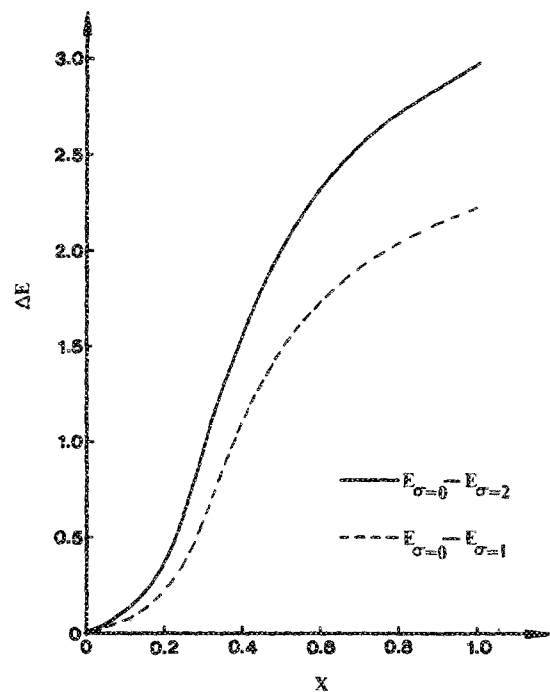


FIG. 6. The shift of the ground-state energy of electron $E_{\sigma=0} - E_{\sigma=1}$ (---) and $E_{\sigma=0} - E_{\sigma=2}$ (—) as functions of Al concentrations x with $L_0 = 100 \text{ \AA}$ and $a_0 = b_0 = L_0/2$.

Figure 7 presents the variations of widths and gaps of the first two conduction minibands as functions of fluctuation parameter σ , with $L_0 = 160 \text{ \AA}$, $a_o = b_o = L_0/2$, and $x = 0.3$. The plot was obtained by an average of up to ten independent groups of a_i, b_i , as we have done previously. Again, the standard deviations are not indicated. The standard deviations are larger for the $n = 2$ subband than for the $n = 1$ subband. We see that the widths of the first two conduction minibands increase as σ increases. From Fig. 7, we can see that the energy values at the zone center (zone edge) for all the minibands decreases (increases) as σ increases. The forbidden gap decreases because of this fluctuation. The width of the first conduction miniband is 0.1 units at $\sigma = 0$, and then expands to about 1.5 units at $\sigma = 2 \text{ \AA}$ and the width of the second miniband expands from 1.5 units to about 5.7 units as σ goes from 0 to 2 \AA .

The conduction- and valence-band offsets Q_c and Q_v are the most important parameters in the calculation of miniband structures of superlattices. In 1974, Dingle, Wiegmann, and Henry²⁰ found 85:15 for the conduction- and valence-band offset ratio. Miller and co-workers¹⁸ deduced a new offset ratio (at $x \sim 0.3$) to be about 60:40 at 1984. This ratio is now widely used. In Fig. 8, we plotted the effective energy gap of heavy holes, $E_{g_{hh}}$, as functions of Q_c for five different fluctuation parameters σ with $L_0 = 100 \text{ \AA}$, $a_o = b_o = L_0/2$, and $x = 0.3$. This reveals how the band structure is affected by the offset ratio. Here, the effective energy gap represents the minimum energy required for producing excitons with neglecting the Coulomb interaction between electrons and holes. If we define

$$\Delta E_g(\sigma) = E_g(\sigma = 0) - E_g(\sigma),$$

we can see from Fig. 8 that $\Delta E_g(\sigma)$ increases as Q_c increases

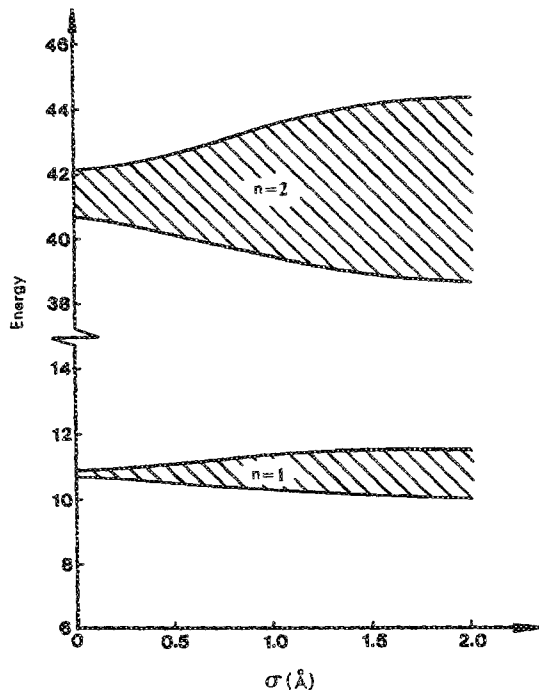


FIG. 7. The first two allowed conduction minibands (shaded area) and minigaps as functions of fluctuation parameter σ with $L_0 = 160 \text{ \AA}$, $a_o = b_o = L_0/2$, and $x = 0.3$.

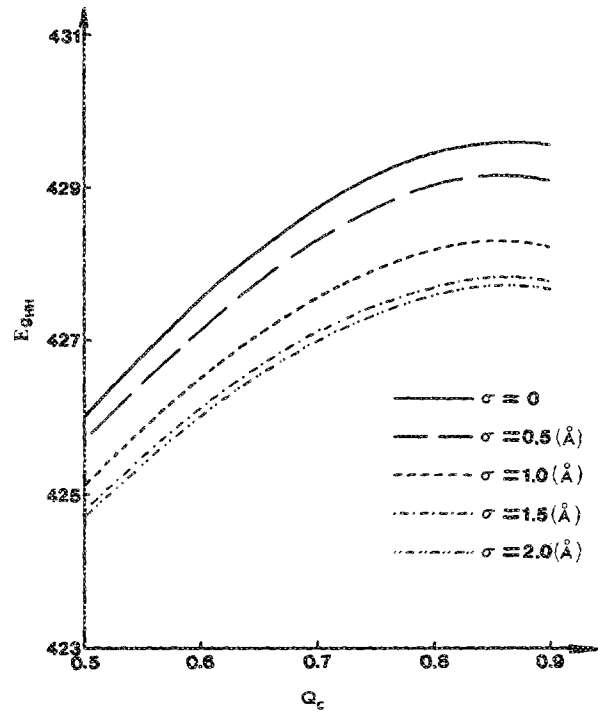


FIG. 8. Effective energy-gap of heavy holes as a function of Q_c , the conduction-band offset, for five different fluctuation parameters σ with $L_0 = 100 \text{ \AA}$, $a_o = b_o = L_0/2$, and $x = 0.3$.

for all σ . $\Delta E_g(\sigma)$ increases almost linearly with Q_c for a fixed value of σ .

We can see from Fig. 8 that Q_c varies widely for a fixed energy value, due to the periodic disorder. This causes difficulty in determining the offset ratio by comparing experimental results to calculations. This may be the reason that the later works favor the lower value of the $Q_c:Q_v$ split because σ should be smaller at the present time due to the availability of more advanced technologies. The above discussion is valid only for superlattices (or multiple quantum well heterostructures). In addition, the above argument is deduced from the results of heavy-hole excitons. The band offset ratio is mainly deduced from the experimental results of heavy-hole excitons.

Figure 9 is the same plot as Fig. 8, but for light holes. $\Delta E_g(\sigma)$ for light-hole excitons has the same behavior as for the heavy holes. $\Delta E_g(\sigma)$ increases as Q_c increases. From the results of Figs. 8 and 9 we can write an effective energy gap for the heavy- and light-hole excitons as

$$E_{g_{hh}}(Q_c, \sigma = 0) = E_{g_{hh}}(Q_c + \Delta, \sigma = \sigma_0), \quad (13a)$$

$$E_{g_{lh}}(Q_c, \sigma = 0) = E_{g_{lh}}(Q_c - \Delta', \sigma = \sigma'_0), \quad (13b)$$

where Δ , Δ' , σ_0 , and σ'_0 are the positive constants. Because of the fluctuation, if we try to obtain Q_c by fitting experimental results with the calculations, there is an uncertainty in Q_c from sample to sample. From the experimental results of energies of heavy- and light-holes excitons and comparing with Figs. 8 and 9, and by knowing all other parameters of the superlattice, we can deduce uniquely the band offset ratio and the fluctuation parameter σ .

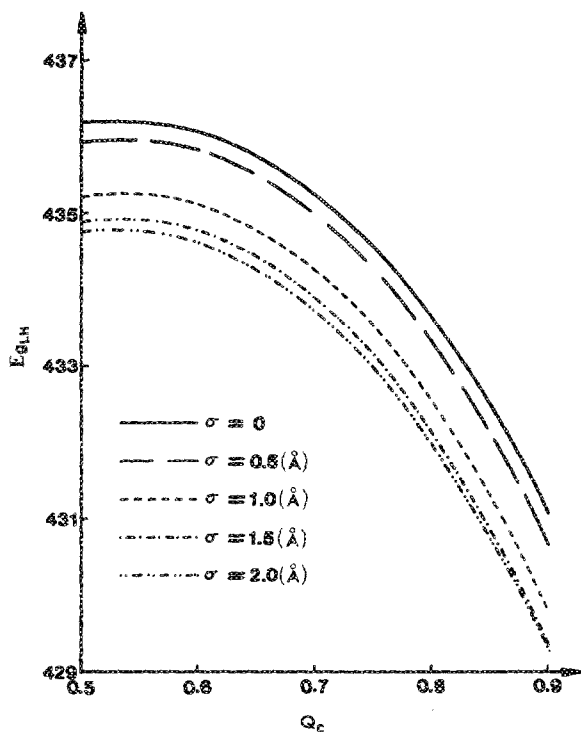


FIG. 9. Effective energy gap of light holes as a function of Q_c , the conduction-band offset, for five different fluctuation parameters σ with $L_0 = 100$ Å, $a_0 = b_0 = L_0/2$, and $x = 0.3$.

IV. CONCLUSIONS

In conclusion, we have studied the effects of the periodic disorder of superlattices to the miniband structures. A random Gaussian distribution of fluctuation in the widths of quantum wells and barriers has been assumed. Under this assumption, the energy values and the standard deviations have been calculated as functions of average period length L_0 , conduction-band offset Q_c , Al concentrations x , and fluctuation parameter σ . The fluctuation in the widths causes a decrease (increase) in the energy of the center of band (edge of band) and expands the widths of the allowed minibands. An asymmetric distribution of electrons about the peak value of the ground-state energy has been predicted. The effective energy gap of heavy and light holes affected by

the periodic disorder were also discussed. Our calculations correspond to the more realistic case of superlattices and is useful for understanding the experimental observations. Although some work has been done for the periodic disorder, many important physical properties, such as electron (hole) mobility, optical emission and absorption, photoluminescence and photoconductivity, and perpendicular transport properties affected by this type of disorder have never been investigated. Further studies have to be done to understand more physical properties of real superlattices.

ACKNOWLEDGMENT

We are grateful to G. Kenning for the critical reading of and comments on the manuscript.

- ¹C. E. C. Wood, in *Physics of Thin Film*, edited by G. Haas and M. H. Francombe (Academic, New York, 1980), Vol. II, p. 35.
- ²See, for example, articles published in *Proceedings of the 4th Molecular Beam Epitaxy Workshop*, edited by H. Morkoç (AIP, New York, 1983).
- ³L. Esaki and R. Tsu, *IBM J. Res. Dev.* **14**, 61 (1970).
- ⁴L. L. Chang, L. Esaki, and R. Tsu, *Appl. Phys. Lett.* **24**, 593 (1974).
- ⁵R. L. Greene and K. K. Bajaj, *Phys. Rev. B* **31**, 91 (1984).
- ⁶H. X. Jiang and J. Y. Lin, in *3rd International Conference on Superlattices, Microstructures, and Microdevices*, 17–20 August 1987, Chicago.
- ⁷B. M. Clemens and J. G. Gay, *Phys. Rev. B* **35**, 9337 (1987).
- ⁸C. Weisbuch, R. Dingle, A. C. Gossard, and W. Weigmann, *J. Vac. Sci. Technol.* **17**, 1128 (1980).
- ⁹C. Weisbuch, R. Dingle, A. C. Gossard, and W. Weigmann, *Solid State Commun.* **38**, 709 (1981).
- ¹⁰T. Hayakawa, T. Suyama, K. Takahashi, M. Kondo, S. Yamamoto, S. Yano, and T. Hijikata, *Appl. Phys. Lett.* **47**, 952 (1985).
- ¹¹E. Merzbacher, *Quantum Mechanics*, 2nd ed. (Wiley, New York, 1970), pp. 73–105.
- ¹²H. X. Jiang and J. Y. Lin, *J. Appl. Phys.* **61**, 624 (1987).
- ¹³R. L. Greene and K. K. Bajaj, *Phys. Rev. B* **31**, 913 (1984).
- ¹⁴W. T. Masselink, Y. C. Chang, and H. Morkoç, *Phys. Rev. B* **28**, 7373 (1983).
- ¹⁵H. J. Lee, L. Y. Juravel, J. C. Wolley, and A. J. Spingthrope, *Phys. Rev. B* **21**, 659 (1980).
- ¹⁶O. Madelung, Ed., *Numerical Data and Functional Relationship In Science and Technology*, Vol. 17 of Landolt-Bornstein (Springer, Berlin, 1982).
- ¹⁷R. C. Miller, A. C. Gossard, D. A. Kleinman, and O. Munteanu, *Phys. Rev. B* **29**, 3740 (1984).
- ¹⁸R. C. Miller, D. A. Kleinman, and A. C. Gossard, *Phys. Rev. B* **29**, 7085 (1984).
- ¹⁹N. F. Mott, *Adv. Phys.* **16**, 49 (1967).
- ²⁰R. Dingle, W. Weigmann, and C. H. Henry, *Phys. Rev. Lett.* **33**, 827 (1974).